AD-A285 854

SHARC-3 CALCULATIONS OF ATMOSPHERIC IR RADIANCE IN THE SOLAR TERMINATOR REGION

DTIC
ELECTE
SEP 3 0 1994
F

S. M. Adler-Golden
M. W. Matthew

Spectral Sciences, Inc.
99 South Bedford Street, #7
Burlington, MA 01803-5169

2 July 1993

Scientific Report No. 4

94-31188

94

"This technical report has been reviewed and is approved for publication"

DEAN F. KIMBALL
Contract Manager
Simulation Branch

WILLIAM A. M. BLUMBERG, Chief
Simulation Branch
Optical Environment Division

ROGER A. VAN TASSEL, Director
Optical Environment Division

REPORT DOCUMENTATION PAGE

Public reporting burden for this collection of information is estimated to average 1 hour per response, including the time for reviewing instructions, searching existing data sources, gathering and maintaining the data needed, and completing and reviewing the collection of information. Send comments regarding this burden estimate or any other aspect of this collection of information, including suggestions for reducing this burden to Washington Headquarters Services, Directorate for Information Operations and Reports, 1215 Jefferson Davis Highway, suite 1204, Arlington, VA 22202-4302, and to the Office of Management and Budget, Paperwork Reduction Project (0704-0188), Washington, DC 20503

1. AGENCY USE ONLY (Leave blank)	2. REPORT DATE 2 July 1993	3. REPORT TYPE AND DATES COVERED Scientific Report #4

4. TITLE AND SUBTITLE
SHARC-3 Calculations of Atmospheric IR Radiance in the Solar Terminator Region

5. FUNDING NUMBERS
C - F19628-91-C-0083
PE- 63215C
PR- S321
TA- 13
WU- AA

6. AUTHOR(S)
S. M. Adler-Golden and M. W. Matthew

7. PERFORMING ORGANIZATION NAME(S) AND ADDRESS(ES)
Spectral Sciences, Inc.
99 South Bedford Street, #7
Burlington, MA 01803-5169

8. PERFORMING ORGANIZATION REPORT NUMBER
SSI-TR-232

9. SPONSORING / MONITORING AGENCY NAME(S) AND ADDRESS(ES)
Phillips Laboratory
29 Randolph Road
Hanscom AFB, MA 01731-3010
Contract Manager: Dean Kimball/GPOS

10. SPONSORING / MONITORING AGENCY REPORT NUMBER
PL-TR-93-2153

11. SUPPLEMENTARY NOTES

12a. DISTRIBUTION / AVAILABILITY STATEMENT

Approved for Public Release; Distribution Unlimited

12b. DISTRIBUTION CODE

13. ABSTRACT (Maximum 200 words)

The Air Force SHARC-3 Atmospheric IR radiance code has been used to simulate CO_2, O_3, and OH limb radiances observed in the solar terminator region during the 1977 SPIRE and 1991 CIRRIS-1A experiments. These calculations represent the first direct comparisons with field data using the new multiple-profiles and multiple-atmospheres features in SHARC-3. The good agreement between the SHARC-3 predictions and the data provide substantial validation of the kinetic and radiation transport models in SHARC as well as the O_3 and H atom profiles from the SHARC Atmosphere Generator.

DTIC QUALITY INSPECTED 3

14. SUBJECT TERMS
infrared   ozone   hydroxyl   limb
atmosphere   shadow   radiation

15. NUMBER OF PAGES
22

16. PRICE CODE

17. SECURITY CLASSIFICATION OF REPORT	18. SECURITY CLASSIFICATION OF THIS PAGE	19. SECURITY CLASSIFICATION OF ABSTRACT	20. LIMITATION OF ABSTRACT
UNCLASSIFIED	UNCLASSIFIED	UNCLASSIFIED	SAR

TABLE OF CONTENTS

LIST OF ILLUSTRATIONS

LIST OF TABLES

1. INTRODUCTION

The Air Force Strategic High-Altitude Radiance Code (SHARC)[1] has been developed to address the strategic requirements for modeling infrared (IR) background radiation in the upper atmosphere. One of the most critical applications is in modeling spatial variability, which is an important effect in the solar terminator (earth shadow edge) region. Two types of effects can occur which lead to spatial radiance variations at the shadow edge. One is a change in molecular number densities due to photochemical processes, such as the photolysis of ozone (O_3). The other is a change in the vibrational excitation with the solar zenith angle. The net result in either case can be a substantial variation in the spectral radiance for many molecular bands, including O_3 (9.6 μm), CO_2 (4.3 μm and 2.7 μm), and OH ($\sim$1.9 μm and $\sim$3.3 μm).

The most recent version of SHARC, SHARC-3, permits accurate modeling of the terminator region through the use of multiple atmospheric profiles corresponding to different solar angles. The spectral radiance may be calculated for an arbitrary line of sight (LOS) passing through up to seven profiles. Interpolation is used to characterize the atmosphere between the solar angles assigned to each profile. The number of profiles is sufficient to accurately describe the characteristics of the shadow edge in any arbitrary view (parallel, perpendicular, or oblique).

In the current investigation, SHARC-3 was used to simulate terminator limb radiances for CO_2, O_3, and OH that correspond to field observations. Dawn terminator data for the CO_2 4.3 μm band were selected from the 1977 SPIRE rocket measurements.[2] New SHARC simulations were performed using an input atmosphere from the SHARC Atmospheric Generator (SAG), a model that utilizes recent climatology databases, empirical models, and theoretical calculations to construct appropriate atmospheric profiles for any desired conditions. The calculated CO_2 radiances are in good agreement with the SPIRE data as well as with simulations performed using GL's line-by-line code RAD.[3] In addition, we have simulated dusk terminator emissions from O_3 and OH measured in the 1991 CIRRIS-1A space shuttle experiment.[4] The reasonable agreement obtained serves to validate both the SHARC code and the SAG solar angle-dependent model for O_3 concentration.

2. CALCULATION METHODS

Two slightly different methods for performing SHARC terminator calculations were used in the current investigation. The CO_2 4.3 μm simulations for SPIRE were performed using a multiple-regions version of SHARC-3. Five atmospheric regions corresponding to different solar angles were defined with explicit geographic boundaries. For convenience, a transformed coordinate system was used in which the scan-center tangent point was placed on the equator and the solar angle served as the longitude coordinate. (See Table 1.) The atmospheric regions were stacked along the equator and bounded by longitude lines; the boundary longitudes were chosen as the mean of the solar angles assigned to the two regions on either side of the boundary. One of the five regions was "extended", i.e., had no boundary. This region was placed at one end of the stack.

For simplicity, the vehicle was regarded as stationary during each spatial scan (this is a good approximation for SPIRE and other rocket experiments). Since the azimuth angle was also fixed during the scan, the entire limb radiance profile for the scan could be mapped out by changing only the LOS tangent height in the SHARC input file. This was done in an automated fashion by running SHARC from an external routine. The routine modified the tangent height in the input file, executed SHARC to compute the LOS

Table 1.   SPIRE Viewing Coordinates in the Transformed System
Used for the Multiple-Regions SHARC Calculations.

Scan	Vehicle Height	Vehicle Longitude	Vehicle Latitude	LOS Azimuth	Tangent Point Height	Tangent Point Longitude	Tangent Point Latitude
1	188.57	92.40	-10.367	26.08	56.60	97.43	0
4	250.09	92.08	-9.922	39.16	87.76	100.07	0
8	279.00	91.80	-0.0675	89.65	158.43	102.73	0
9	266.11	91.24	-2.5958	-75.93	153.63	81.00	0
10	235.97	91.03	-4.9565	-62.13	125.10	81.75	0
11	213.26	90.93	-7.2198	-37.37	131.18	85.45	0

spectral radiance, integrated the result within the selected bandpass, and wrote an output file containing the bandpass radiance and tangent height values.

The O_3 and OH simulations for CIRRIS-1A were performed using the multiple-profiles feature in the July, 1993 release of SHARC-3. Seven atmosphere profiles, corresponding to a 92°-104° solar zenith angle (SZA) range, were specified in a single quiescent region. The actual latitudes and LOS azimuth angles for the experiment were used. The correct placement of the sun was achieved through the choice of input longitude.

The only real difference between using a single profile within multiple regions (in the CO_2 calculations for SPIRE) as opposed to multiple profiles within a single region (in the calculations for CIRRIS-1A) is that in the latter case the vibrational state populations are interpolated along the LOS, whereas in the former case they are constant within each region and change abruptly at the boundaries. For radiators such as CO_2 where the solar angle-dependence of vibrational state populations is gradual, the calculated limb radiances are similar with either approach. With O_3 and OH emissions, which change dramatically over a several-degree solar angle range, the interpolation provided in the multiple-profiles method should give smoother results.

3. RESULTS AND COMPARISONS

3.1 CO_2 4.3 μm

Calculations of the 4.19-4.49 μm bandpass radiance were carried out to simulate the SPIRE "terminator/night" scans 1, 4 and 8 and the "day" scans 9 and 11. For the former, five layers at 2° SZA increments were used, for a total SZA range of 10° along the LOS. This is sufficient for coverage of tangent heights up to 150 km or greater. For scan 8, which looked much farther into the night than the other two, a low-solar-angle extended region was substituted for the daylit extended region used in the scan 1 and scan 4 calculations. For the day scans 9 and 11, which have generally greater East-West ranges, the atmospheric regions were made three and four degrees wide.

3.1.1 CO_2 Vibrational Temperatures

To obtain some insight into the SZA-dependence of the CO_2 excitation and the convergence properties of the calculations, we tabulated the vibrational temperature of the main isotope (00011) state (associated with the ν_3 cold band) for each atmospheric region. As expected, there is a general decrease with increasing SZA (Figure 1). The temperatures for one set of altitudes, around 119 km, track one another closely. High temperatures in region 1 are followed by approximately level temperatures in the darker regions.

A similar trend appears at lower altitudes around 91 km, but the temperatures do not track. The small fluctuations appearing at this altitude are statistical, stemming from the finite number of Monte Carlo "photons" used in the NEMESIS routine that calculates the vibrational populations. Ten thousand photons per vibrational band were used to develop the Figure 1 results, and should be adequate for most applications. If this number is decreased to N = 500, much larger fluctuations occur, as in Figure 2. The relative magnitudes of the fluctuations in these two figures are consistent with the statistical $\sqrt{N}$ scaling, as expected.
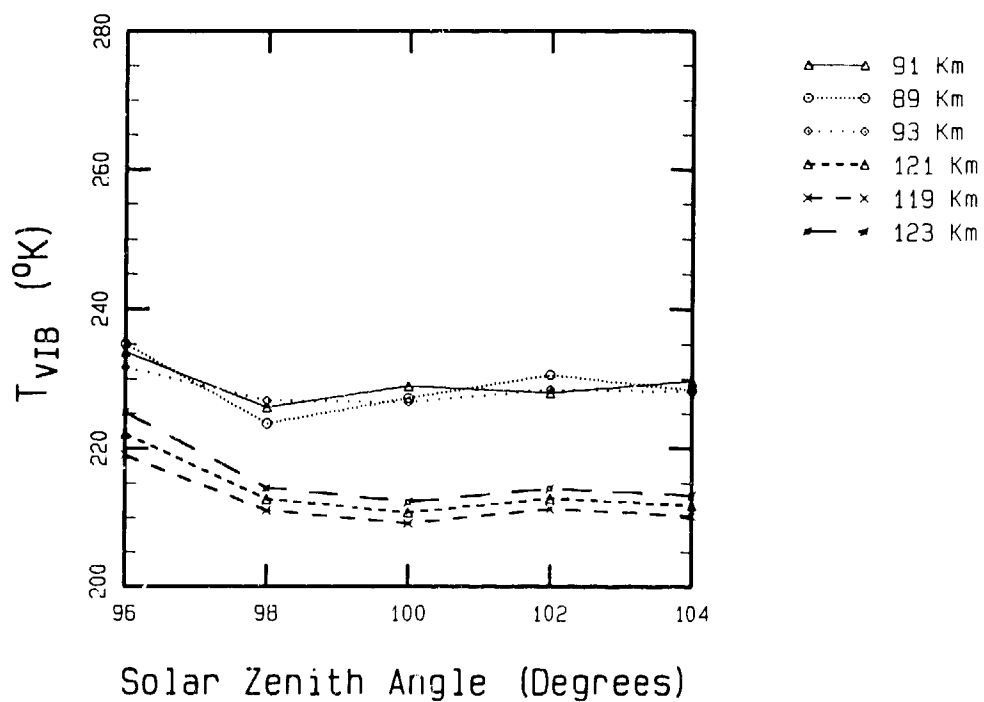
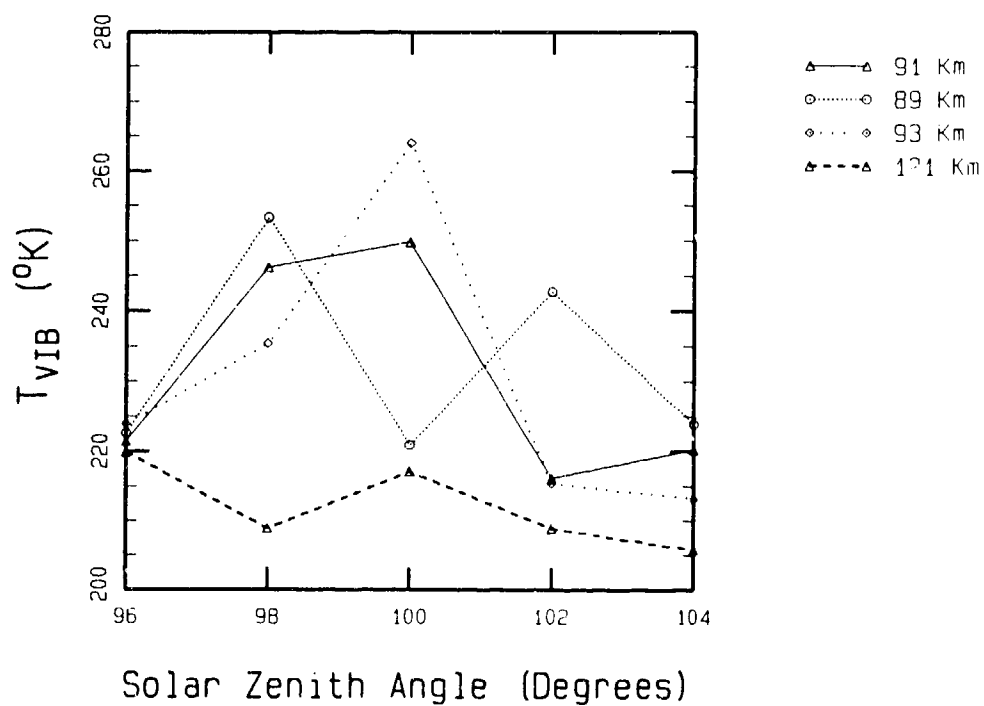Figure 1. Solar-Angle Dependence of the CO_2 (00011) State Vibrational Temperature Computed Using 10,000 NEMESIS Photons.

Figure 2. Same as in Figure 1 But Using 500 NEMESIS Photons.

3.1.2 Radiance Profiles

The 4.3 μm radiance profiles from SHARC appear in Figure 3 along with the SPIRE data. Since the data display significant scatter not correlated with SZA, data for similar angles have been collected into two sets, corresponding to day and night sides of the terminator. The scan 1 data are very limited and are not shown. Two SHARC profiles are shown for each set to indicate the sensitivity of the calculations to the SZA. No differences are found between the various nighttime calculations below 100 km, where strong atmospheric absorption of sunlight leads to total shadow. In other cases, minor differences are found. The agreement between the SHARC calculations and the SPIRE data is seen to be within the data scatter. As can be seen in Fig. 3, the SHARC calculations for 99 and 107 SZA are essentially nighttime except at the higher altitudes.
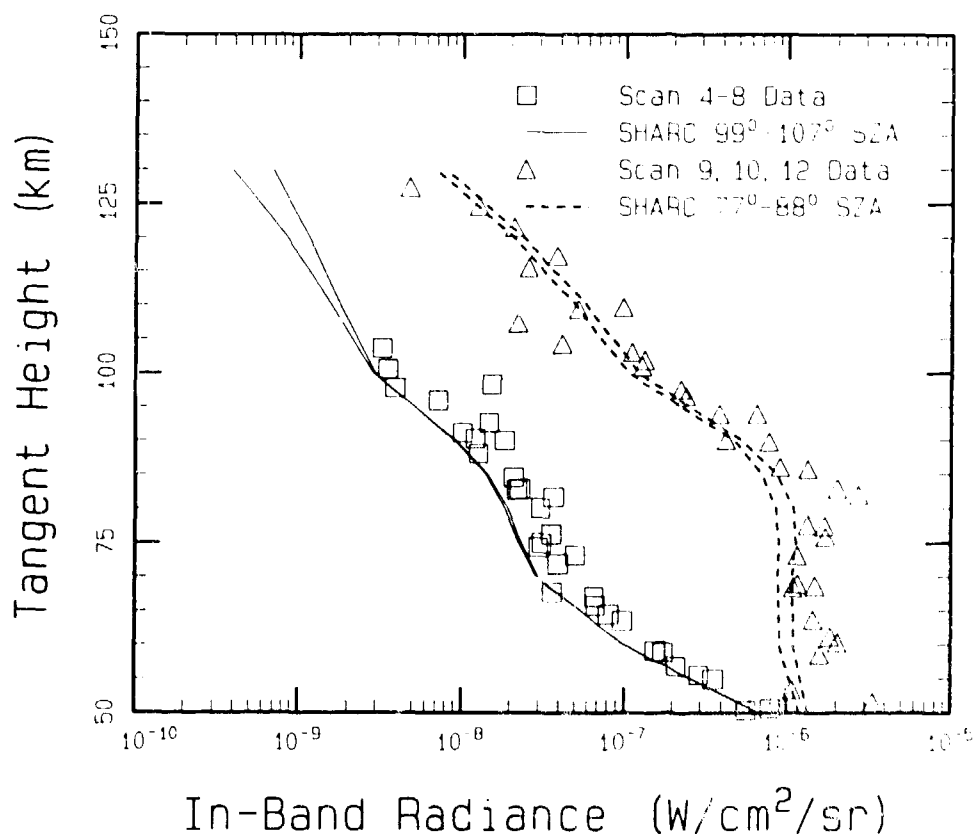

Figure 3.   Comparison of 4.3 μm Limb Radiance Measurements from the SPIRE Rocket Experiment with SHARC-3 Simulations.

Preliminary SHARC calculations have also been performed to simulate CIRRIS 1A data, which have better signal-to-noise. The results, which will be reported in the future, indicate agreement to within a factor of 2 over the 50 to 125 km tangent height range. The SHARC radiances tend to be lower, particularly at the higher tangent heights. An underprediction of this magnitude has also been found by Wintersteiner and co-workers at nighttime using a different radiation code (RAD)[3] with similar kinetic mechanisms.

3.2 O_3 9.6 μm

In contrast with CO_2, the variation in ozone radiance at the solar terminator is due to an abrupt change in concentration. Thus, the SHARC terminator results depend critically on how the ozone concentration profile changes with solar zenith angle in the model atmospheres. A discussion of the ozone profile derivation, excerpted from the SHARC Atmosphere Generator (SAG) documentation,[5] is presented below.

3.2.1 Derivation of Ozone Concentration Profile

The ozone profile is based on a combination of the NRL trace species climatology database[5] and a photochemical equilibrium model, described below. The NRL database contains daytime mixing ratios and night/day ratios, and is used below 72 km. The latitude range is restricted to $\pm 60°$ to avoid interpolation difficulties associated with the onset of continuous polar day or night. The photochemical model is used at 80 km and above, and the two regions are connected by logarithmic interpolation.

The photochemical equilibrium model accounts for ozone formation from O atoms and destruction via H atom and O atom reactions (the former yielding OH) and solar photolysis. The inputs are the photolysis rate and the temperature, N_2, O_2, O, and H profiles, which, as discussed in the SAG documentation, are based almost entirely on the MSISE-90 model.[7] Along with the standard three-body recombination reaction, a two-body radiative association term is also included, and has a significant and increasing impact above 100 km. The value of the rate constant, 8×10^{-21} cm^3/molec/s, is estimated from rate constants for formation and relaxation of the O_2-O complex[8] and from ν_3 band Einstein coefficients. It is almost certainly an upper limit. We feel that it is safer to risk overestimating the ozone than to underestimate it. Furthermore, any overestimation from this 2-body channel would be reduced by the presence of certain $O_2^* + O_2$ reactions that have been proposed to form ozone[9] but which are not presently included in SAG.

The transition between day and night profiles is handled using a simple empirical model that approximates the terminator behavior in the time-dependent calculations of Rodrigo et al.,[10] which were performed for mid-latitude (45°) equinox conditions above 60 km. The transition is made by linearly interpolating over a 5° range of SZA computed for 0.075 hr earlier; the 0.075 hr (4.5 min) difference accounts for the approximate photochemical lag time. The midpoint of the interpolation region is taken to vary linearly with altitude at the rate of 0.12° per km.

3.2.2 Ozone Profile Comparisons

Figure 4 compares the daytime and nighttime concentrations from SAG and from the NRL climatology. The SAG and NRL climatology results differ above 72 km where the transition to the photochemical model is made in SAG, but the difference is generally a factor of two or less. According to the photochemical model, above 80 km ozone is destroyed almost exclusively by reaction with H atoms. Much of the difference between the NRL and SAG nighttime profiles may have to do with inaccuracy in the MSISE-90 H atom profile used by SAG. Recent observations[11] suggest that the MSISE-90 profile may be somewhat low, especially near 80 km. Further investigation of this issue is warranted.

The temporal behavior of the SAG ozone concentrations in the dawn and dusk terminator regions is shown in Figures 5a and 5b. Comparing them with Rodrigo et al.'s calculations in Figures 6a and 6b, it is seen that while the absolute concentrations from SAG are different, particularly at night, both the day/night transition times (indicating the shadow edge location) and the slopes of the curves (indicating the sharpness of the edge) are very similar throughout the 60-100 km altitude range. At lower altitudes, both the NRL climatology database and our own survey of literature measurements indicate that, contrary to Rodrigo's calculations, the diurnal variation of ozone is very small. Therefore, any error in the terminator edge model will be negligible below 60 km.

In conclusion, the SAG model should provide a good empirical description of ozone concentration in the daytime, nighttime, and terminator region.
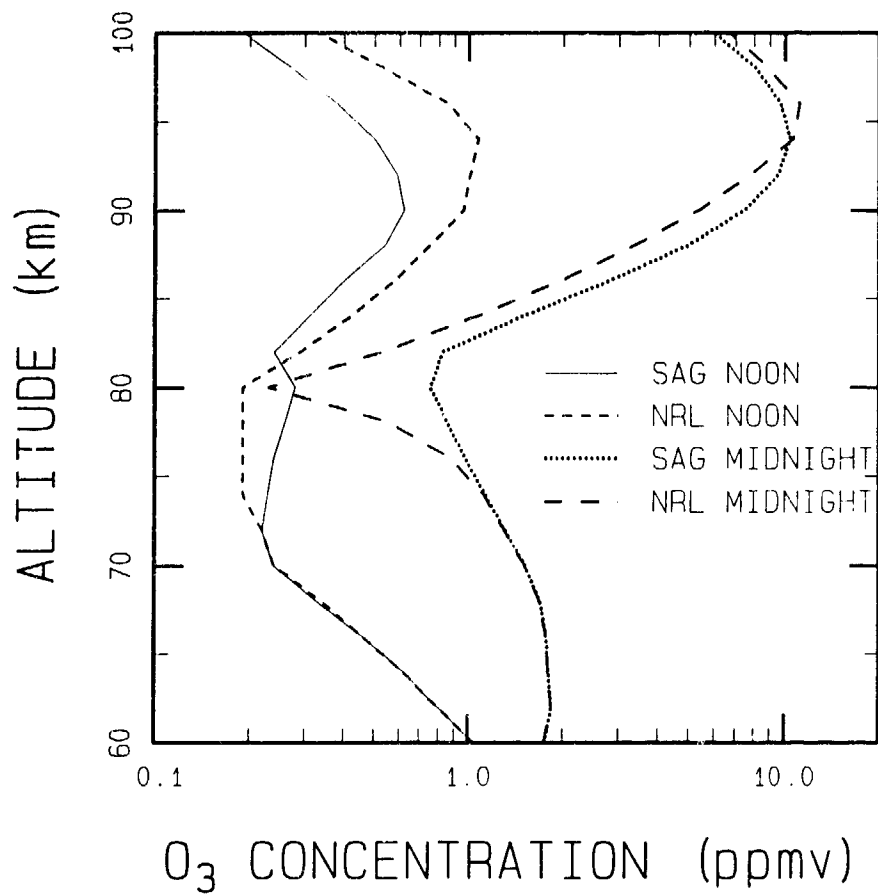
Figure 4. Comparison of SAG Model and NRL Climatology Ozone Concentrations for Fall Equinox, 45° N Latitude, Moderate-Activity Conditions.
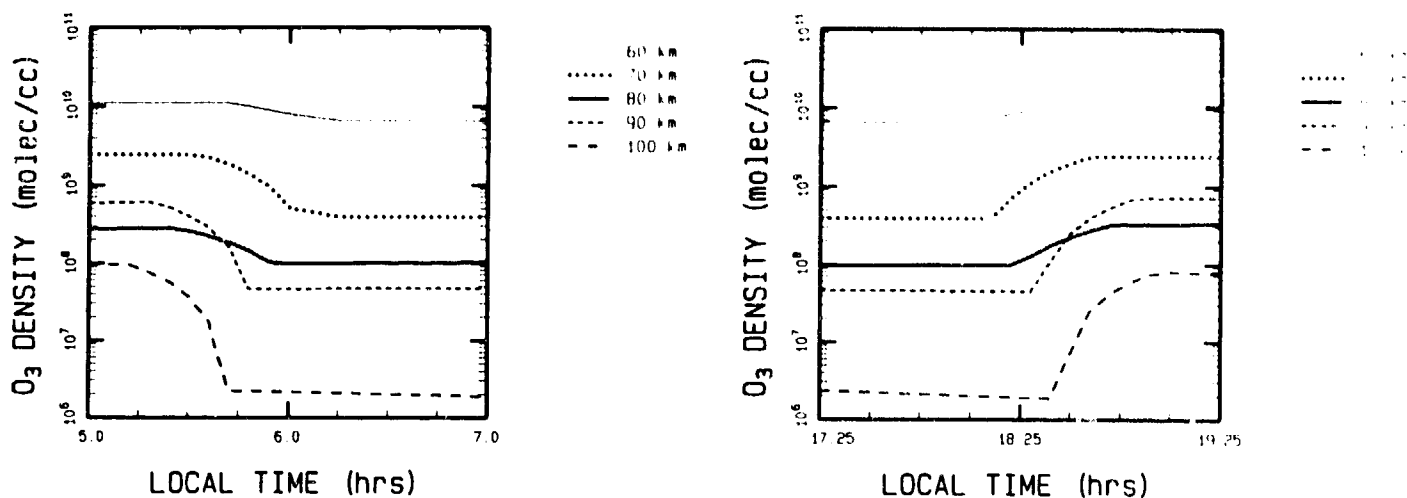
Figure 5.   Time-Dependent Ozone Concentrations from SAG in the Solar Terminator Regions for Fall Equinox, 45° N Latitude, Moderate-Activity Conditions.
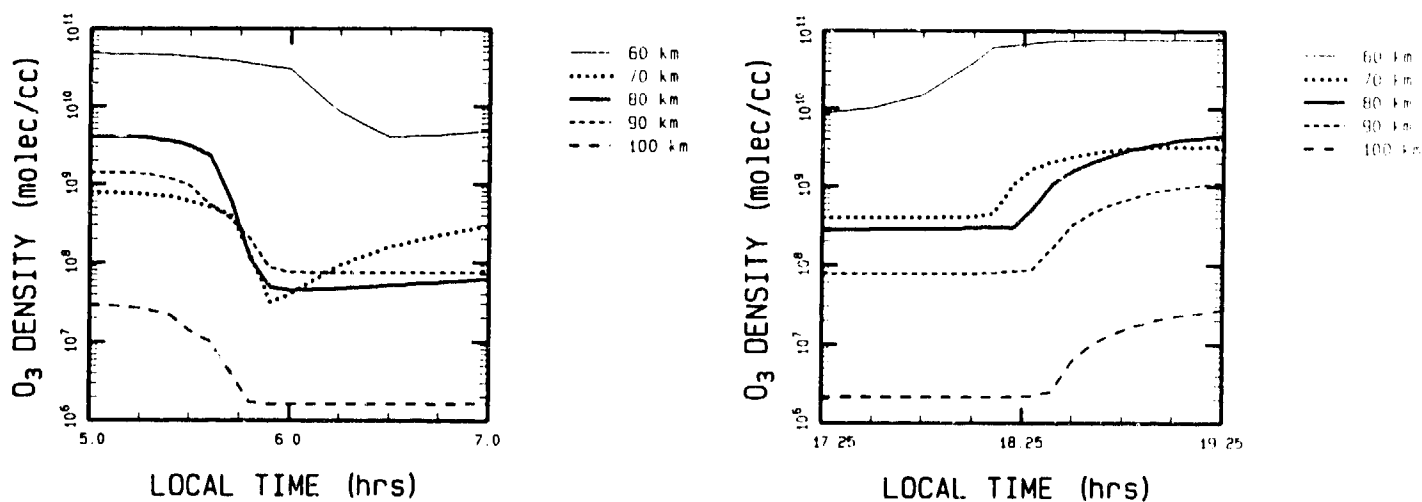

Figure 6.   Time-Dependent Ozone Concentrations from Rodrigo et al.[10] in the Solar Terminator Regions for Fall Equinox, 45° N Latitude.

3.2.3 Terminator O_3 Radiance

SHARC calculations were performed to simulate selected data from the CIRRIS-1A experiment on O_3 ν_3 radiance in the dusk terminator.[12] The data were taken from a horizontal scan near 20° S latitude during Block PC11G, when a SZA range of 93° to 101° was covered with nearly constant elevation and azimuth angles. During this period, two radiometer detectors, numbered 1-4 and 1-6, acquired data at 89 km and 81 km tangent heights, respectively, in the 8.0-11.9 μm bandpass. The LOS was nearly parallel to the terminator.

The data and SHARC simulations are shown in Figure 7. The SHARC simulations show a smaller altitude dependence on the night side and slightly underestimate the day side radiance, but on the whole they agree reasonably with the data. The agreement is better at 81 km, which is closer to the peak of the ozone emission, than at 89 km. The differences on the night side may have to do with a mismatch between the calculated and actual ozone peak altitude, which averages around 83 km in CIRRIS-1A nighttime measurements but can fluctuate by several km. For these particular data, the peak appears to be several km lower than average. At 89 km, the scale height of the emission is very steep, so that a small change in the peak altitude can have a large effect on the radiance. Uncertainties in the CIRRIS-1A pointing could also explain some or most of the differences. The tangent height uncertainty is estimated to be 1 to 2 km for these data.
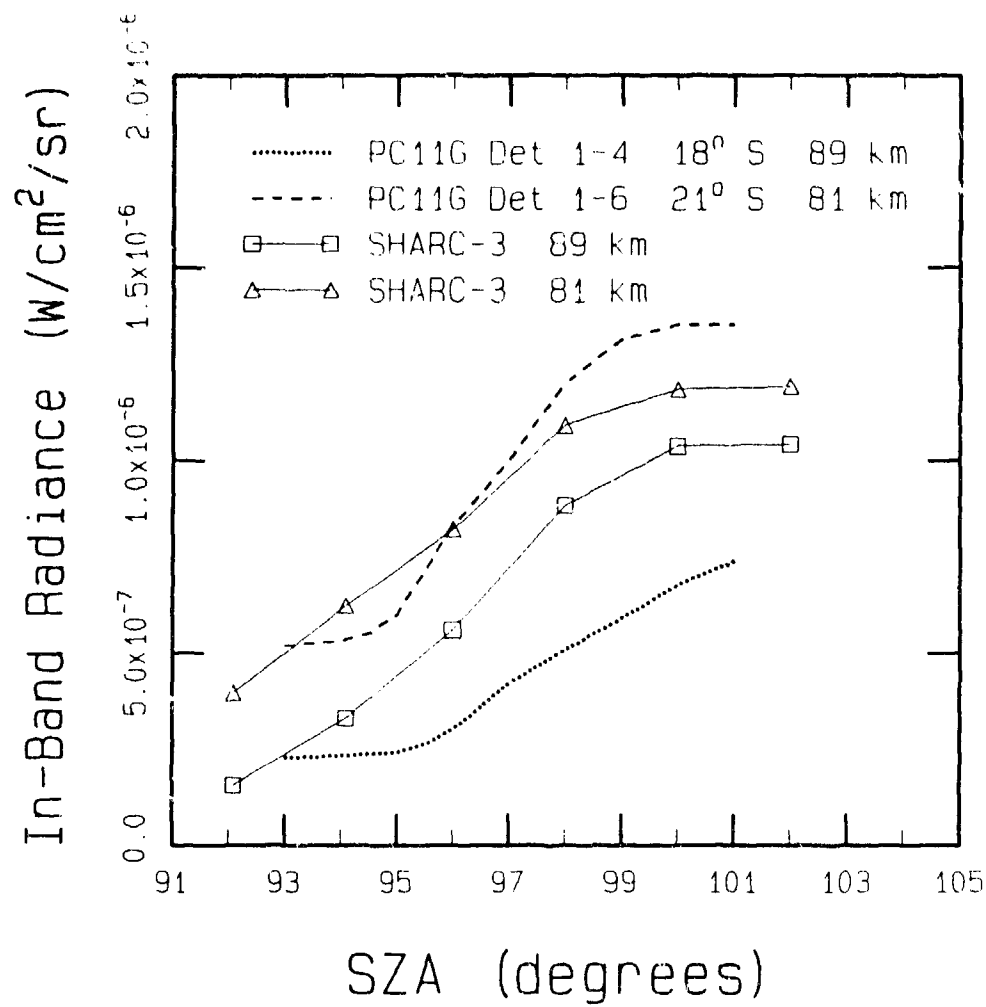
Figure 7. Calculated (SHARC-3) and Observed (CIRRIS-1A) $O_3(\nu_3)$ Limb Radiances at the Dusk Terminator.

3.3 OH $\Delta V = 1$

The OH $\Delta V = 1$ Meinel band emission above 80 km is generated from the H + O_3 reaction. The H and O_3 concentration profiles have been discussed in Section 3.2.1. The OH emission is expected to show a similar terminator behavior as the O_3 emission, since the H atom concentration should not vary across the terminator at these altitudes. Not surprisingly, we find the SHARC/CIRRIS-1A data comparison for OH to be similar to that for O_3.

3.3.1 Terminator OH Radiance

Figure 8 shows 2.5-3.4 μm bandpass data from CIRRIS-1A that were taken simultaneously with the O_3 data of Figure 7. The small quantity of emission at the lowest SZA's is from a blend of OH($\Delta V = 1$) and CO_2 2.7 μm bands; the increase starting around 94° is ascribed entirely to OH(V) formed from the increasing quantity of ozone. The SHARC calculation yields slightly more OH emission than observed, but the difference is well within the variability of the OH emissions and the pointing uncertainty. The solar angle dependence of the data is also reproduced quite well; the location of the terminator edge appears to be accurate to within 2° or less of SZA.

Since the concentration of ozone derived from the photochemical model is inversely proportional to the H atom concentration, the quantity of OH emission at night does not depend on the assumed H atom profile. However, it does depend on the O atom recombination rate, and hence on the O atom concentration as well as the mechanism and rate constants for OH(V) deactivation. Future refinements of the OH(V) kinetics in SHARC will provide a more precise relationship between the OH emissions and the recombination rate, so that these emissions could be used for deriving accurate O atom profiles in the mesopause region.
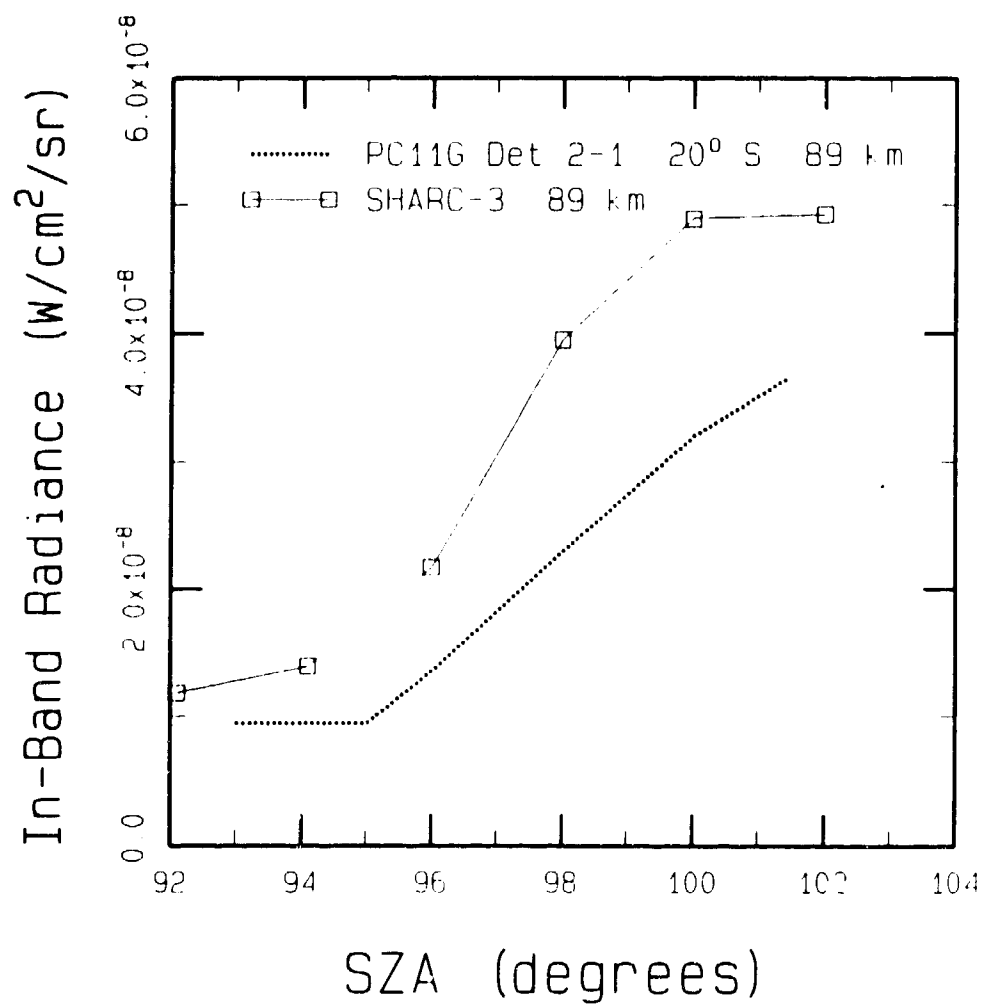
Figure 8. Calculated (SHARC-3) and Observed (CIRRIS-1A) OH($\Delta V = 1$) Limb Radiances at the Dusk Terminator.

4. CONCLUSIONS

The SHARC-3 atmospheric IR radiance code has been used to simulate limb radiances for CO_2, O_3, and OH in the solar terminator region that correspond to observations from the 1977 SPIRE and 1991 CIRRIS-1A experiments. These calculations represent the first direct comparisons with field data using the new multiple-profiles and multiple-atmospheres features in SHARC-3. The good agreement between the calculations and the data provide substantial validation of the kinetic and radiation transport models in SHARC as well as the O_3 and H atom profiles from the SHARC Atmosphere Generator (SAG).

Similar comparisons are underway using additional data from CIRRIS-1A and/or other experiments to more fully investigate these emissions over a wider range of viewing conditions and to investigate other radiators and bandpasses of interest.

5. ACKNOWLEDGEMENTS

6. REFERENCES

1.   (a) R. L. Sundberg, J. W. Duff, L. S. Bernstein, J. H. Gruninger, P. K. Acharya, D. C. Robertson, M. W. Matthew, A. Berk, and S. M. Adler-Golden, "SHARC, A Comprehensive Non-Equilibrium Infrared Radiation Model for the Upper Atmosphere," Rpt. No. SSI-TR-228 under Air Force Contract F19628-91-C-0083, June 1993, PL-TR-93-2135.
   (b) R. D. Sharma, A. J. Ratkowski, R. L. Sundberg, J. W. Duff, L. S. Bernstein, P. K. Acharya, J. H. Gruninger, D. C. Robertson, and R. J. Healey, "Description of SHARC, the Strategic High-Altitude Radiance Code," Environ. Res. Pap., 1036, Geophysics Laboratory, Hanscom AFB, MA (1989), GL-TR-89-0229, ADA213806.

2.   A. T. Stair Jr., R. D. Sharma, R. M. Nadile, D. J. Baker, and W. F. Grieder, "Observations of Limb Radiance with Cryogenic Spectral Infrared Rocket Experiment," J. Geophys. Res., 90, 9763 (1985).

3.   P. P. Wintersteiner, R. A. Joseph, and A. J. Paboojian, "High-Altitude Non-Equilibrium Infrared Emission Models," Arcon Corporation, Final Report under Contract F19628-86-C-0118; GL-TR-90-0311, Geophysics Laboratory, Hanscom AFB, MA (1990), ADA232503.

4.   D. R. Smith, W. A. M. Blumberg, R. M. Nadile, S. J. Lipson, E. R. Huppi, and N. B. Wheeler, "Observation of High-N Hydroxyl Pure Rotation Lines in Atmospheric Emission Spectra by the CIRRIS-1A Space Shuttle Experiment," Geophys. Res. Lett., 19, 593 (1992).

5.   P. K. Acharya, D. C. Robertson, and A. Berk, "Upgraded Line-of-Sight Geometry Package and Band Model Parameters for MODTRAN," Scientific Report No. 5 under Contract F19628-89-C-0128; PL-TR-93-2127, Phillips Laboratory/GPOS, Hanscom AFB, MA (1993). ADA280952

6.   M. E. Summers, W. J. Sawchuck, and G. P. Anderson, "Model Climatologies of Trace Species in the Atmosphere," Annual Review Conference on Atmospheric Transmission Models, Phillips Laboratory, Hanscom AFB, MA, June, 1992.

7.   A. Hedin, "Extension of the MSIS Thermosphere Model Into the Middle and Lower Atmosphere," J. Geophys. Res., 96, 1159 (1991).

8.   H. Hippler, R. Rahn, and J. Troe, "Temperature and Pressure Dependence of Ozone Formation Rates in the Range 1-1000 Bar and 90-370 K," J. Chem. Phys., 93, 6560 (1990).

9.   J. Shi and J. R. Barker, "Odd Oxygen Formation in the Laser Irradiation of O_2 at 248 nm: Evidence for Reactions of O_2 in the Herzberg States With Ground State O_2," J. Geophys. Res., 97, 13039 (1992).

10.   R. Rodrigo, M. J. Lopez-Gonzalez, and J. J. Lopez-Moreno, "Variability of the Neutral Mesospheric and Lower Thermospheric Composition in the Diurnal Cycle," Planet. Space Sci., 39, 803 (1991).

11. R. J. Thomas, "Atomic Hydrogen and Atomic Oxygen Density in the Mesopause Region: Global and Seasonal Variations Deduced from Solar Mesosphere Explorer Near-Infrared Emissions," J. Geophys. Res., 95, 16457 (1990).

12. D. R. Smith, R. M. Nadile, E. Richards, R. Hegblom, and R. Gibson, "Diurnal Variability of IR Emission Profiles Near the Terminator as Observed by the CIRRIS 1A Experiment From the Space Shuttle," presented at the AGU Spring Meeting, Montreal, May 12-15, 1992.